Vol. 66, No. 11, November 2014, pp 2976–2988
DOI 10.1002/art.38809

Endoplasmic Reticulum Degradation–Enhancing α-Mannosidase–like Protein 1 Targets Misfolded HLA–B27 Dimers for Endoplasmic Reticulum–Associated Degradation

David B. Guiliano,[1] Helen Fussell,[2] Izabela Lenart,[3] Edward Tsao,[3] Darren Nesbeth,[3] Adam J. Fletcher,[3] Elaine C. Campbell,[4] Nasim Yousaf,[3] Sarah Williams,[4] Susana Santos,[5] Amy Cameron,[4] Greg J. Towers,[3] Paul Kellam,[3] Daniel N. Hebert,[6] Keith G. Gould,[7] Simon J. Powis,[4] and Antony N. Antoniou[3]

Objective. **HLA–B27 forms misfolded heavy chain dimers, which may predispose individuals to inflammatory arthritis by inducing endoplasmic reticulum (ER) stress and the unfolded protein response (UPR). This study was undertaken to define the role of the UPR-induced ER-associated degradation (ERAD) pathway in the disposal of HLA–B27 dimeric conformers.**

Methods. **HeLa cell lines expressing only 2 copies of a carboxy-terminally Sv5-tagged HLA–B27 were generated. The ER stress–induced protein ER degradation–enhancing α-mannosidase–like protein 1 (EDEM1) was overexpressed by transfection, and dimer levels were monitored by immunoblotting. EDEM1, the UPR-associated transcription factor X-box binding protein 1 (XBP-1), the E3 ubiquitin ligase hydroxymethylglutaryl-coenzyme A reductase degradation 1 (HRD1), and the degradation-associated proteins derlin 1 and derlin 2 were inhibited using either short hairpin RNA or dominant-negative mutants. The UPR-associated ERAD of HLA–B27 was confirmed using ER stress–inducing pharamacologic agents in kinetic and pulse chase assays.**

Results. **We demonstrated that UPR-induced machinery can target HLA–B27 dimers and that dimer formation can be controlled by alterations to expression levels of components of the UPR-induced ERAD pathway. HLA–B27 dimers and misfolded major histocompatibility complex class I monomeric molecules bound to EDEM1 were detected, and overexpression of EDEM1 led to inhibition of HLA–B27 dimer formation. EDEM1 inhibition resulted in up-regulation of HLA–B27 dimers, while UPR-induced ERAD of dimers was prevented in the absence of EDEM1. HLA–B27 dimer formation was also enhanced in the absence of XBP-1, HRD1, and derlins 1 and 2.**

Conclusion. **The present findings indicate that the UPR ERAD pathway can dispose of HLA–B27 dimers, thus presenting a potential novel therapeutic target for modulation of HLA–B27–associated inflammatory disease.**

HLA–B27 is strongly associated with a group of inflammatory arthritic conditions known as the spondyloarthritides, with ankylosing spondylitis (AS) representing the prototypical presentation (1,2). Up to 90–95% of patients with AS are positive for HLA–B27, but despite the fact that this genetic association has been known for almost 4 decades, the disease mechanism remains poorly

Dr. Fussell's work was supported by Arthritis Research UK (project grant 17222). Dr. Lenart's work was supported by Arthritis Research UK (studentship 17868). Dr. Campbell's work was supported by the Chief Scientist Office of the Scottish Government. Dr. Towers' work was supported by the Wellcome Trust (Senior Biomedical Fellowship). Dr. Hebert's work was supported by the US Public Health Service (grant GM086874). Dr. Antoniou's work was supported by Arthritis Research UK (fellowship 15293).

[1]David B. Guiliano, PhD: University College London and University of East London, London, UK; [2]Helen Fussell, PhD: Colindale Blood Centre, London, UK; [3]Izabela Lenart, PhD, Edward Tsao, PhD, Darren Nesbeth, PhD, Adam J. Fletcher, PhD, Nasim Yousaf, PhD, Greg J. Towers, PhD, Paul Kellam, PhD, Antony N. Antoniou, PhD: University College London, London, UK; [4]Elaine C. Campbell, PhD, Sarah Williams, PhD, Amy Cameron, PhD, Simon J. Powis, PhD: University of St. Andrews, Fife, UK; [5]Susana Santos, PhD: INEB–Instituto de Engenharia Biomedica, Porto, Portugal; [6]Daniel N. Hebert, PhD: University of Massachusetts, Amherst; [7]Keith G. Gould, DPhil: Imperial College London, London, UK.

Drs. Guiliano and Fussell contributed equally to this work.

Address correspondence to Antony N. Antoniou, PhD, University College London, Division of Infection and Immunity/Centre of Rheumatology, Rayne Building, 5 University Street, London WC1E 6JF, UK. E-mail: anthony.antoniou@ucl.ac.uk.

Submitted for publication November 5, 2013; accepted in revised form July 29, 2014.

understood. Genome-wide genetic screening studies have identified a number of other genes contributing to AS, but none have yet fully explained the disease process (3). One current theory linking HLA–B27 to AS involves the predisposition of HLA–B27 heavy chain to misfold and form non-native heavy chain dimeric structures (4). HLA–B27 dimers have been correlated with disease in the rat model of spondyloarthritis (5). Dimers may interact aberrantly with immunoreceptors at the cell surface or act within the environment of the endoplasmic reticulum (ER) to induce cellular stress responses, potentially leading to the onset of proinflammatory responses (6,7).

Major histocompatibility complex (MHC) class I molecules present unique protein folding challenges to the ER quality control machinery, and HLA–B27 is particularly prone to misfolding, forming disulfided bonded dimers (8). Misfolding proteins within the ER can induce the unfolded protein response (UPR), which is a cellular stress response initiating transcriptional changes whose function is to restore ER homeostasis (9,10). There are 3 main effector molecules of the UPR: activating transcription factor 6, inositol-requiring enzyme 1 (IRE-1), and PERK, which reside within the ER. All are maintained in an inactive state by the ER-resident chaperone BiP (10–12). One of the most potent transcriptional changes induced by the UPR occurs following the oligomerization and autophosphorylation of IRE-1. Phosphorylated IRE-1 can splice cytosolically located X-box binding protein 1 (XBP-1) messenger RNA by excising a 26-nucleotide intronic sequence, generating the transcription factor XBP-1 spliced (XBP-1s) (13). XBP-1s can activate chaperones to enhance cellular folding capacity and/or proteins involved in degradation of misfolding substrates (14).

ER degradation–enhancing α-mannosidase–like protein 1 (EDEM1) was originally cloned as an ER stress–induced gene (15), which is targeted by XBP-1s (14). EDEM1 overexpression studies have demonstrated a role of this protein in the degradation of misfolded proteins. EDEM1 is thought to handle misfolded proteins in concert with the ER chaperone calnexin and the UPR-induced XBP-1 target E3 ubiquitin ligase hydroxymethylglutaryl-coenzyme A reductase degradation 1 (HRD1)–suppressor of Lin12–like 1 (SEL1) complex (16–18). Together with the E2 ubiquitin–conjugating enzyme UBE2J1 they were shown to participate in the degradation of misfolded MHC class I heavy chains at steady state (19). Very recently, a role of EDEM1 in the MHC class I pathway has also been demonstrated (20), although its interaction with HLA–B27 was not investigated.

In the current study we demonstrated that EDEM1 participates in the degradation of HLA–B27 dimers under conditions of ER stress. This degradation pathway requires XBP-1 and HRD1. Of note, our data indicate that the ER stress–induced ERAD pathway is a potential route for therapeutic intervention in HLA–B27–associated diseases.

MATERIALS AND METHODS

Cell lines and antibodies. Cells were maintained in Dulbecco's modified Eagle's medium (Invitrogen) supplemented with 10% fetal bovine serum (FBS; Globepharm) and penicillin/streptomycin (D10 media) and maintained in a 5% CO_2 37°C incubator. The Invitrogen Flp-In system was used to generate isogenic HeLa lines stably expressing HLA class I constructs. HeLa cells with 2 integrated copies of the pFRT/lacZeo plasmid were identified by Southern blot analysis. Clone H2Z was β-galactosidase positive and Zeocin resistant. HLA class I constructs for expression were cloned into the pEF5/FRT/V5-D-TOPO vector. The relevant Flp recombinase target site–containing expression plasmid was cotransfected, together with the Flp recombinase-expressing plasmid pOG44, into H2Z cells and selected using hygromycin B. Recombinants were identified by the lack of β-galactosidase expression and Zeocin sensitivity, thus generating stable isogenic lines containing 2 copies of HLA class I expression constructs driven by the human elongation factor 1α promoter or cytomegalovirus promoter. The following antibodies were used: anti-V5 (pK; Serotec), anti-FLAG, anti-EDEM1, and horseradish peroxidase (HRP)–conjugated anti-rabbit monoclonal antibody (Sigma), and HRP-conjugated goat anti-mouse antibody (Dako). Antibodies ME1 (detecting conformational-specific HLA–B27) and 4E (detecting HLA–B35) were kind gifts from Dr. J. Neefjes (Amsterdam, The Netherlands) and P. Lehner (Cambridge, UK), respectively.

Transient transfection. HeLa and HEK 293T cells were plated at 1×10^5 and 5×10^5 cells/well, respectively, and transfected with complementary DNA (cDNA) expression constructs and JetPrime PEI (Polyplus Transfection) or FuGene (Promega), respectively, according to the recommendations of the manufacturers.

Immunoprecipitation and immunoblotting. For EDEM1 immunoprecipitation experiments, HeLa cells expressing HLA–B*27:05 were transfected with FLAG-tagged EDEM1, incubated with 20 m*M* *N*-ethylmaleimide/phosphate buffered saline (NEM/PBS; pH7.4), lysed in 1% digitonin lysis buffer, immunoprecipitated with anti-FLAG antibody, and washed in 1% digitonin buffer. For analysis of EDEM1 binding to MHC class I molecules, 293T cells cotransfected with EDEM1-FLAG and HLA class I molecules were treated with 20 m*M* NEM, lysed in 1% Nonidet P40 (NP40) lysis buffer, and immunoprecipitated with anti-FLAG antibody.

For immunoblotting, samples were resolved by nonreducing sodium dodecyl sulfate–polyacrylamide gel electrophoresis (SDS-PAGE), transferred onto nitrocellulose (BA85;

Schleicher & Scheull), blocked for 1 hour with 5% skim milk powder in PBS/0.1% Tween, and then incubated with antibodies. Images were revealed by chemiluminescence using SuperSignal Femto reagents (Pierce).

Knockdown analysis. For XBP-1 knockdown, transductions with short hairpin RNA (shRNA)–expressing lentiviral vector (pCSBX/pIG) targeting XBP-1 (shXBP-1) were performed as previously described (21). An equivalent control vector expressing an shRNA targeting luciferase (shLuc) was generated using the same methodology. HEK 293T cells were transfected with p8.91, pMDG, and the shRNA-expressing lentiviral vector genome, using FuGene 6. Samples showing high levels of viral transduction (>90% green fluorescent protein positive by fluorescence-activated cell sorting) were processed and immunoblotted. For HRD1 and EDEM1 knockdown, previously described 19-mer oligonucleotides matching HRD1 cDNA (19) or EDEM1 cDNA (22) were incorporated into DNA oligos that were cloned into pSIREN-RetroQ shRNA expression vector (Clontech) and sequence verified. HEK 293T cells were transfected with plasmids encoding Moloney murine leukemia virus Gag-Pol (pCMVi), vesicular stomatitis virus G Env (pMDG), and pSIREN-RetroQ–shHRD1 or shEDEM1 to produce pseudotyped virus-like particles. Supernatants were harvested 48 hours after transfection.

Chemical inhibitor, ER stress induction, and dimer half-life assays. HeLa cells expressing HLA–B*27:05 were incubated at 1×10^5 cells/well with various concentrations of kifuensine (KIF; Calbiochem) or DMSO as control and harvested 18 hours later. HeLa–B27 cells were incubated with various concentrations of tunicamycin (TUN), thapsigargin (TPG), and MG132 for ER stress studies or with 50 μM cycloheximide for half-life analyses. Equal numbers of cells were harvested, treated with NEM, and lysed in 1% NP40 lysis buffer. Protein loading was normalized by cell number or MTT assay.

Monocyte-derived dendritic cells (DCs) and quantitation. After full local ethics committee review/approval and informed consent were obtained, peripheral blood mononuclear cells were isolated by centrifugation of whole blood over Histopaque (Sigma). Monocytes adhered to plastic for 2 hours (in RPMI/10% FBS) were cultured with 50 ng/ml

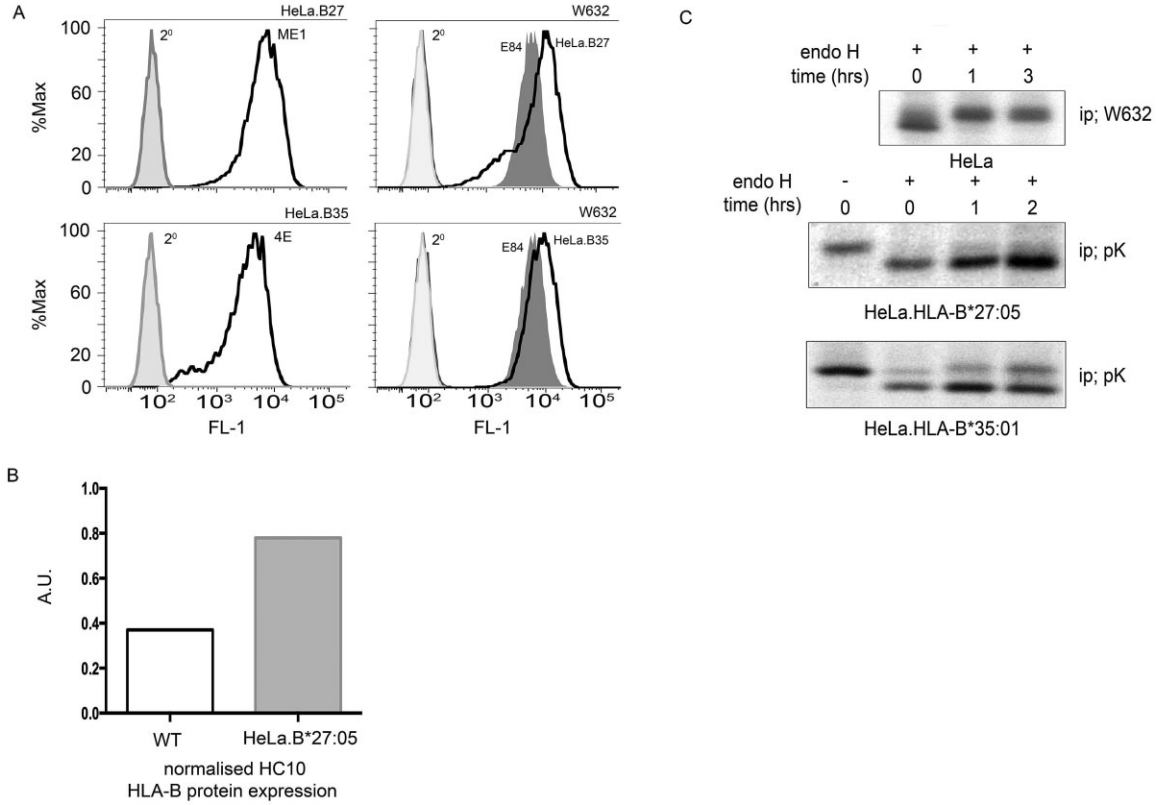

Figure 1. HLA–B27 expression and maturation in HeLa cells. **A,** HLA–B27 and HLA–B35 are expressed efficiently at the cell surface. HeLa–B27.Sv5 and HeLa–B35.Sv5 cells were analyzed by flow cytometry with antibodies ME1 and 4E, respectively. HeLa–B27 cells, HeLa–B35 cells, and mock-transfected controls (E84) expressed antibody W632–reactive major histocompatibility complex (MHC) class I molecules. **B,** Quantitation of HLA–B alleles using HC10 antibody revealed approximately twice as much HLA–B expression in HeLa–B27.Sv5 cells compared to wild-type (WT) HeLa cells. **C,** HeLa cells process MHC class I molecules efficiently. Pulse chase analysis of endogenous MHC class I molecules using antibody W632 followed by endoglycosidase H (Endo H) digestion revealed that MHC class I molecules mature within 1 hour. Pulse chase of HeLa–B27.Sv5 cells using the anti-Sv5 pK antibody showed that little Endo H–resistant material was acquired during 2 hours of chase, whereas in control HeLa–B35.Sv5 cells, rapid acquisition of Endo H resistance was observed. IP = immunoprecipitation.

interleukin-4 and 50 ng/ml granulocyte–macrophage-colony-stimulating factor (R&D Systems). DCs were allowed to differentiate for 5 days and treated with 100 ng/ml lipopolysaccharide (LPS; Sigma). Cell lysates were analyzed by SDS-PAGE and immunoblotted for MHC class I heavy chain (with HC10) and for HRD1, and developed with SuperSignal Femto chemiluminescence reagents. HRD1 and B27D values were generated from the Integrated Density in ImageJ (National Institutes of Health). All values were then normalized to β–actin. For quantitation of HLA–B alleles, lysates were analyzed for HC10 reactivity and values generated as described above.

Pulse chase analysis. Cells were serum starved for 15 minutes and labeled with ^{35}S-Cys/Met (300 μCi) for 15 minutes. Radiolabel was removed and cells resuspended in D10. For ER stress or pharmacologic treatment, drugs were added at the point of chase. At each time point equal numbers of cells were removed, treated with 20 m*M* NEM (pH 7.4) on ice for 20 minutes, lysed in 1% NP40, and immunoprecipitated for MHC class I. Prior to resolution by nonreducing SDS-PAGE, samples were treated with endoglycosidase H (Endo H) for 1 hour at 37°C.

RESULTS

Direct association of EDEM1 with aberrant MHC class I conformers. To investigate the role of EDEM1 in the processing of HLA–B27 dimers, we used isogenic HeLa cells expressing 2 copies of either Sv5 C-terminally tagged HLA–B27 (HeLa–B27.Sv5) or Sv5 C-terminally tagged HLA–B*35:01 (HeLa–B35.Sv5) under the control of the E1Fα promoter. The latter was used as a control HLA–B allele that does not form disulfide-linked dimers.

Flow cytometric analysis of HeLa–B27.Sv5 and –B35.Sv5 with antibodies ME1 and 4E, respectively, revealed efficient cell surface expression of these MHC class I molecules (Figure 1A), while W632 staining demonstrated that all lines expressed endogenous MHC class I molecules. We assessed the amount of HLA–B proteins expressed by HeLa compared to HeLa–B27.Sv5 by immunoblotting with HC10. Quantitative analysis revealed approximately twice as much HLA–B expression in HeLa–B27.Sv5 cells compared to wild-type HeLa cells (Figure 1B), consistent with the additional 2 copies of HLA–B27. We previously showed that HLA–B27 exhibits slow maturation kinetics (23), and pulse chase analysis of HeLa–B27.Sv5 confirmed the slow maturation kinetics compared to HLA–B35, as demonstrated by the acquisition of Endo H–resistant material within 2 hours. Pulse chase analysis of endogenous W632-reactive MHC class I molecules in wild-type HeLa cells (Figure 1C) and analysis of HLA–B35 demonstrated that MHC molecules can be processed efficiently and rapidly by HeLa cells and that the slow kinetics of HLA–B27 are independent of cell line expression.

Next we performed experiments in which EDEM1 expression was enhanced as well as experiments in which it was inhibited, to assess its role in the processing of HLA–B27 dimers. The HeLa–B27.Sv5 line expresses 3 distinct dimer populations which, as we have previously shown, correspond to dimers in different redox states (24). Overexpression of EDEM1 resulted in a modest reduction in the levels of all HLA–B27 dimer populations (Figure 2A), while depletion of EDEM1 expression led to enhancement of all 3 dimer populations (Figure 2B). As both of these differences in dimer levels were observed at steady state, we then induced ER stress in the absence of EDEM1, using TPG. Immunoblotting revealed that HLA–B27 dimers were more abundant in EDEM1-depleted cells (Figure 2B).

We used a pharmacologic approach to further verify that EDEM1 can participate in the degradation of aberrant HLA–B27 dimers. HLA–B27 dimers were enhanced after treatment with KIF, which inhibits ERAD and the interaction of EDEM1 with the HRD1–SEL1 degradation complex (18,25,26). In addition, the dimer complexes displayed a small increase in molecular weight (Figure 2C), characteristic of the retention of high-mannose groups due to the inhibition of class I α-mannosidase activity. The monomers for both HLA–B27 and HLA–B35 were also resolved as 2 closely migrating bands in the presence of KIF (Figure 2C), which may represent a mannosylated heavy chain and/or intermediates of HLA heavy chains prior to ERAD. KIF treatment could potentially affect dimer formation by altering the maturation rate of HLA–B27. However, pulse chase analysis in the presence of KIF revealed no alteration in HLA–B27 maturation rates (Figure 2C).

To determine whether EDEM1 can directly associate with different forms of HLA–B27, EDEM1-FLAG cDNA was either transfected into HeLa–B27.Sv5 cells or cotransfected with HLA–B*27:05 cDNA into HeLa cells. Following immunoprecipitation of EDEM1, immunoblotting for HLA–B27 with antibody HC10 demonstrated the preferential association of HLA–B27 dimers compared to monomeric HLA–B27 (Figure 2D). These data suggest that EDEM1 can both associate with MHC class I dimeric heavy chains and modulate their levels.

Misfolded MHC class I heavy chains interact with EDEM1 in a glycan-independent manner. We next investigated whether EDEM1 can associate directly with misfolded monomeric heavy chains. In a cell-based binding assay, 293T cells were cotransfected with EDEM1-FLAG and C-terminally Sv5-tagged wild-type HLA–B*27:05 or with similarly tagged misfolding HLA–B27 molecules that had the conserved structural cys-

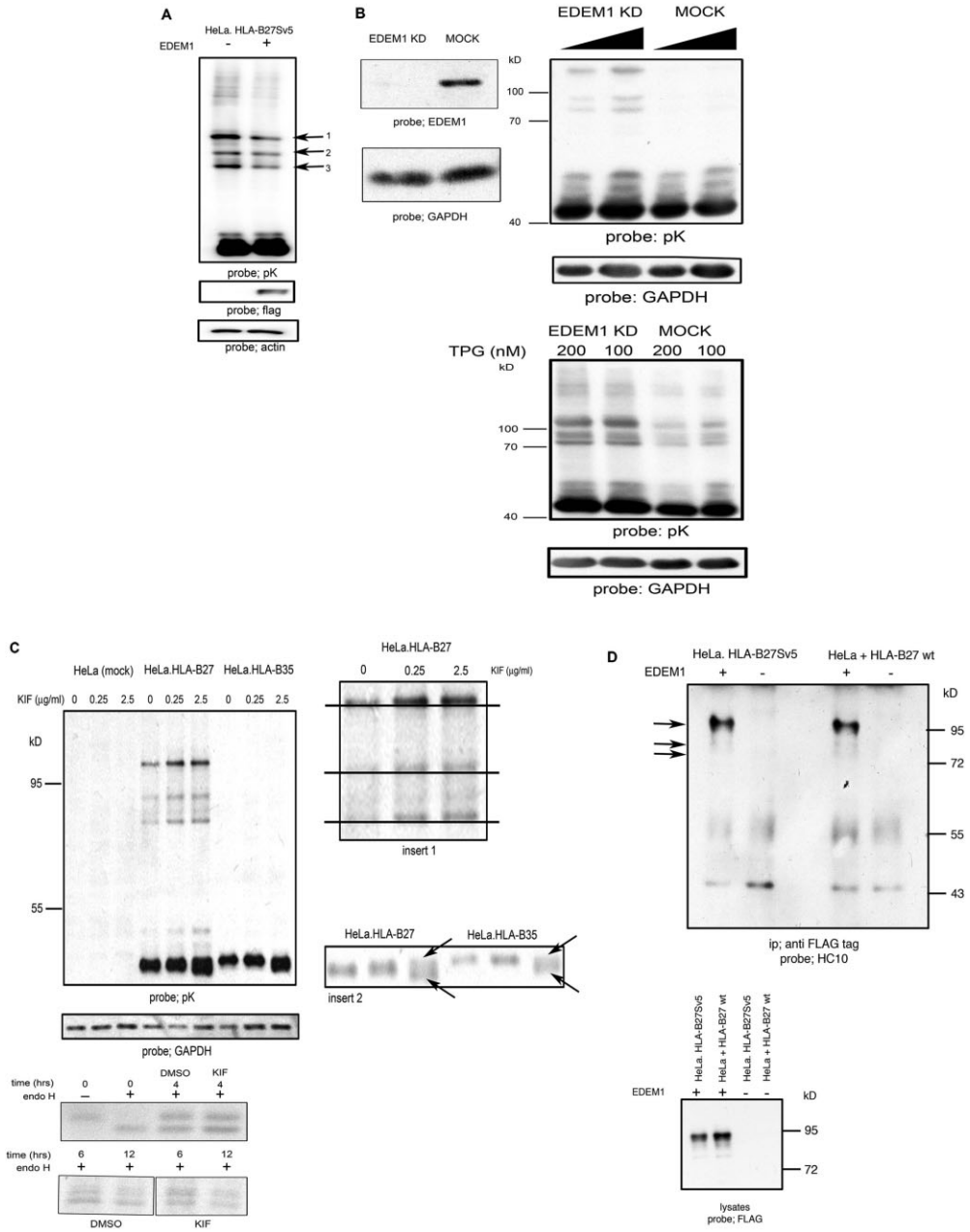

Figure 2. Endoplasmic reticulum (ER) degradation–enhancing α-mannosidase–like protein 1 (EDEM1) modulates HLA–B27 dimers. **A,** Overexpression of EDEM1 can enhance HLA–B27 dimer degradation. HeLa–B27 cells were transfected with EDEM1-FLAG, lysed, and immunoblotted for major histocompatibility complex (MHC) class I heavy chain. **Arrows 1, 2,** and **3** indicate HLA–B27 dimers. Lysates immunoblotted with anti-FLAG exhibited EDEM1 expression. **B,** Left, Short hairpin RNA (shRNA) inhibition (knockdown [KD]) of EDEM1 expression in HeLa–B27 cells prevented HLA–B27 dimer ER-associated degradation when compared to mock transduction with a control scrambled shRNA. Right, HLA–B27 dimers were resistant to ER stress–induced degradation following EDEM1 knockdown. **C,** Top, Increasing concentrations of kifuesine (KIF) led to enhanced detection of dimers, as determined by immunoblotting of HeLa–B27.Sv5 cells; immunoblotting for GAPDH revealed equal loading. Insert 1 demonstrates that with increasing KIF concentrations, the high molecular weight dimers exhibit small changes in molecular weight; **arrows** in insert 2 indicate that at 2.5 μg/ml KIF, the monomers of both HLA–B27:05 and HLA–B*35:01 can be resolved as a doublet. Bottom, KIF did not alter the maturation rate of HLA–B27. HeLa–B27.Sv5 cells were radiolabeled and chased in the presence of KIF or vehicle control DMSO. **D,** HLA–B27 ER resident dimers preferentially associate with EDEM1. Top, HeLa–B27.Sv5 cells were transfected with EDEM1-FLAG or HeLa cells were cotransfected with HLA–B27 and EDEM1-FLAG, and cell lysates were immunoprecipitated (IP) with an anti-FLAG tag antibody and immunoblotted for MHC class I heavy chain. Bottom, Immunoblotting of lysates with anti-FLAG from HeLa and HeLa–B27.Sv5 cells transfected with EDEM1 revealed equal levels of EDEM1 expression. TPG = thapsigargin; Endo H = endoglycosidase H; WT = wild-type.

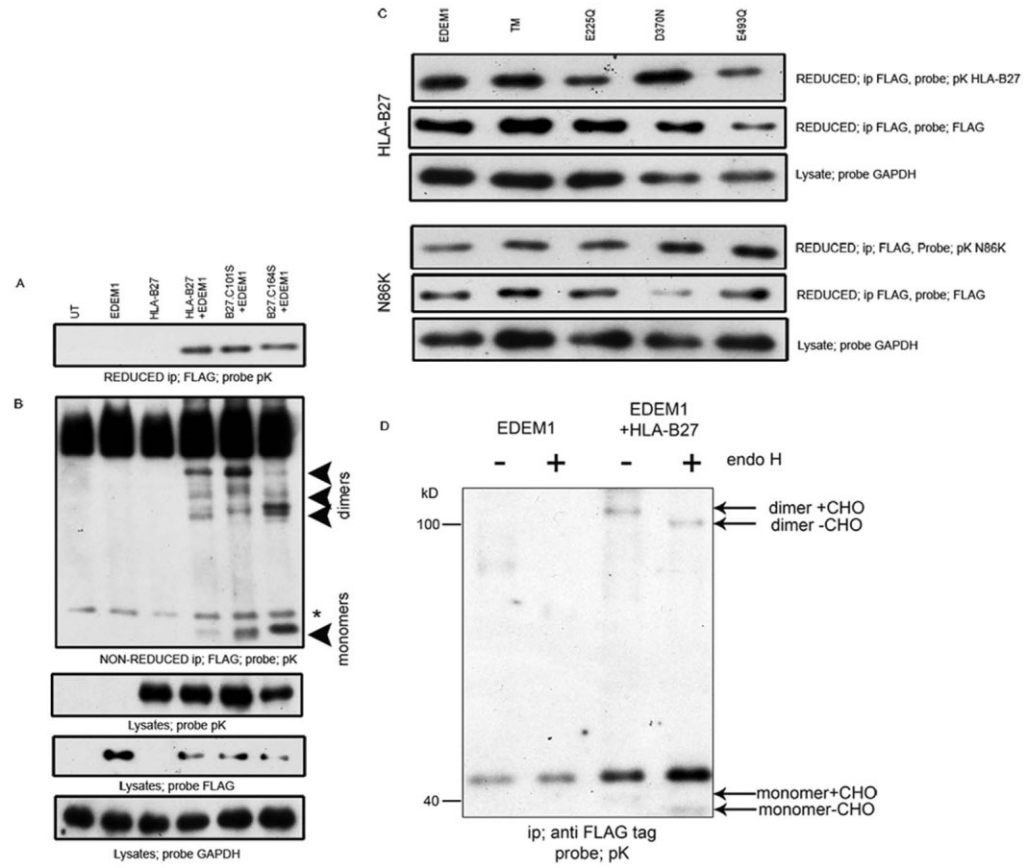

Figure 3. EDEM1 associates with dimeric and monomeric MHC class I conformers. **A,** MHC class I molecules are detected only when coexpressed with EDEM1. HEK 293T cells were cotransfected with EDEM1 and HLA–B27.Sv5 with or without the misfolding mutants B27.C101S and B27.C164S. Lysates were immunoprecipitated for anti-FLAG, resolved by reducing sodium dodecyl sulfate–polyacrylamide gell electrophoresis (SDS-PAGE), and immunoblotted for V5 using pK antibody. **B,** Both monomers and dimers can be detected in association with EDEM1. Immunoprecipitates similar to those described in **A** were resolved by nonreducing SDS-PAGE and immunoblotted with pK antibody. Note that dimeric structures are preferentially detected in the presence of WT HLA–B27 and the C101S mutant. **Asterisk** denotes a nonspecific background band. **C,** EDEM1 associates with HLA–B27 in a glycosylation-independent manner. HEK 293T cells were cotransfected with EDEM1, E493Q, D370N, E225Q, or a triple mutant (TM) contaning all 3 mutations, along with WT HLA–B27 or a glycosylation site–deficient mutant (N86K). Lysates were immunoprecipitated with anti-FLAG, resolved by reducing SDS-PAGE, and probed with pK antibody. **D,** EDEM1 was immunoprecipitated and Endo H digested following cotransfection with HLA–B27 in 293T cells, and immunoblotting for MHC class I heavy chain was performed. UT = untreated; CHO = carbohydrate (see Figure 2 for other definitions).

teines of the α2 domain mutated to serines at position 101 (C101S) or 164 (C164S). The structural HLA–B27.C101S monomer misfolds but retains the ability to extensively dimerize, and the C164S mutant exhibits enhanced levels of misfolded monomer with a reduced ability to dimerize (23). Therefore, with the use of these mutants we could determine whether EDEM1 associates with dimeric and/or monomeric conformations. Twenty-four hours after transfection, 293T cells were harvested, treated with 20 m*M* NEM, and lysed in 1% NP40. Lysates were immunoprecipitated for EDEM1 using an anti-FLAG antibody and resolved by reducing SDS-PAGE.

Immunoblotting for HLA–B27 with the anti-Sv5 pK antibody indicated that wild-type HLA–B*27:05 and the C101S and C164S mutants could be coimmunoprecipitated with EDEM1 (Figure 3A). When resolved under nonreducing conditions, fewer monomeric wild-type HLA–B27 heavy chains interacted with EDEM1. It is likely that this pool would contain both correctly folded and misfolded monomers, whereas both C101S and C164S monomer heavy chain pools would all be classified as misfolded. Interestingly, C101S predominantly associated as a dimer with EDEM1, while C164S exhibited an altered dimeric conformation, but could associate with EDEM1 both as a monomer and as a dimer (Figure 3B).

To determine whether the EDEM1 mannosidase-like domain was important in HLA–B27 heavy chain recognition, we used a series of EDEM1 mutants, i.e., E225Q, E493Q, and D370N, whose acidic active site residues within the mannosidase-like domain had been mutated to neutral amino acids that abolish glycan-dependent substrate binding. In addition, we used a triple mutant of this domain, E225Q/D370N/E493Q. To further address the requirement of glycan binding, we used a glycosylation site–deficient mutant of HLA–B27, N86K. In a cell-based binding assay we coexpressed wild-type EDEM1 or the 4 EDEM1 mutants with HLA–B27 or the B27.N86K mutant. Cells were treated with NEM, lysed in 1% NP40, and immunoprecipitated for EDEM1. Immunoblotting for MHC class I heavy chains demonstrated that both wild-type and N86K HLA–B27 could be coimmunoprecipitated with all EDEM1 mutants (Figure 3C).

HLA–B27 dimers can be ER resident and expressed at the cell surface. To determine which pool of dimers was associated with EDEM1, we subjected the EDEM1-associated HLA–B27 molecules to digestion with Endo H. Immunoblotting revealed that following Endo H digestion, the dimeric population associating with EDEM1 exhibited an apparent lower molecular weight, correlating with the removal of glycans from ER-resident dimers (Figure 3D). Furthermore, under these experimental overexpression conditions we additionally detected monomeric HLA–B27, which was also susceptible to Endo H digestion (Figure 3D).

The above-described results show that the EDEM1–MHC class I interaction is not dependent on glycosylation of the substrate or the glycan binding site of EDEM1. They also demonstrate that EDEM1 binds with ER-resident dimers and misfolding monomeric heavy chains.

HLA–B27 dimer ERAD requires the XBP-1 pathway and HRD1 and can use derlins 1 and 2. As EDEM1 is a target gene for the potent UPR transcription factor XBP-1s (14,27), we predicted that heavy-chain dimer degradation would require an intact XBP-1 pathway. We transduced HeLa–B27.Sv5 cells with a lentivirus expressing an shRNA targeting XBP-1, and immunoblotting revealed that in the absence of XBP-1, HLA–B27 dimers were more prevalent (Figure 4A).

EDEM1 and HRD1 are targets for XBP-1s induction (14,27), and EDEM1 can associate with the HRD1–SEL1 degradation complex (18). We therefore wished to confirm the role of HRD1 in HLA–B27 dimer degradation. We hypothesized that inhibition of HRD1 expression should prevent ERAD of HLA–B27 dimers. HeLa-B27.Sv5 cells were infected with a retrovirus expressing an shRNA construct targeting HRD1. Immunoblotting for HLA–B27 dimers revealed a large accumulation of dimers and larger aggregates (Figure 4A). We then wished to determine how inhibition of XBP-1 would affect HRD1 and EDEM1 expression. XBP-1 inhibition led to a reduction in steady-state levels of HRD1 but did not greatly affect EDEM1. We next subjected HeLa cells that were either mock transduced or had undergone XBP-1 inhibition to treatment with the ER stress–inducing agent TPG. Both HRD1 and EDEM1 could be induced with increasing concentrations of TPG; however, in the absence of XBP-1, neither of these proteins could be significantly induced (Figure 4B). Therefore, inhibition of XBP-1 can prevent the induction of EDEM1 and HRD1 under stress conditions.

To determine the physiologic significance of the above-described pathway for HLA–B27 dimer degradation, we analyzed HLA–B27 dimer and HRD1 levels in cells from HLA–B27–positive AS patients. Monocyte-derived DCs from peripheral blood were stimulated with LPS and MHC class I dimer, and HRD1 levels analyzed by immunoblotting. Intriguingly, HRD1 levels were consistently higher in patient-derived DCs compared to DCs from HLA–B27–positive healthy controls (Figure 4C), suggesting that HRD1 may regulate HLA–B27 dimer levels in AS patient cells.

The derlin proteins have been postulated to be part of putative degradation pores and act as adaptors for ERAD substrates (28). Derlin 1 is involved in glycoprotein US11–mediated retrotranslocation of monomeric MHC class I molecules (29), while derlin 2 links EDEM1 with the ERAD p97 component. Furthermore, derlins 1–3 can be induced by ER stress (30). As derlin 1 has a role in MHC class I ERAD and derlin 2 has been demonstrated to associate with EDEM1, we wished to determine whether HLA–B27 dimer degradation could be affected by derlin 1 and/or derlin 2. We used derlin 1 and 2 green fluorescent protein fusion proteins, which act as dominant-negative proteins for their respective products (29). The inhibition of derlins 1 and 2 by their respective dominant-negative proteins resulted in enhanced dimers (Figure 4D). Thus, HLA–B27 dimers can be targeted for degradation via an XBP-1–dependent pathway, and their degradation involves the E3 ubiquitin ligase HRD1 and the putative adaptor proteins derlin 1 and/or derlin 2.

Long life of HLA–B27 heavy-chain dimers. HLA–B27 dimers have been postulated to be pathogenic and to participate in inflammatory arthritic disease (5). We initially wished to determine the half-life of HLA–B27 dimers. The longevity of HLA–B27 dimers has not been

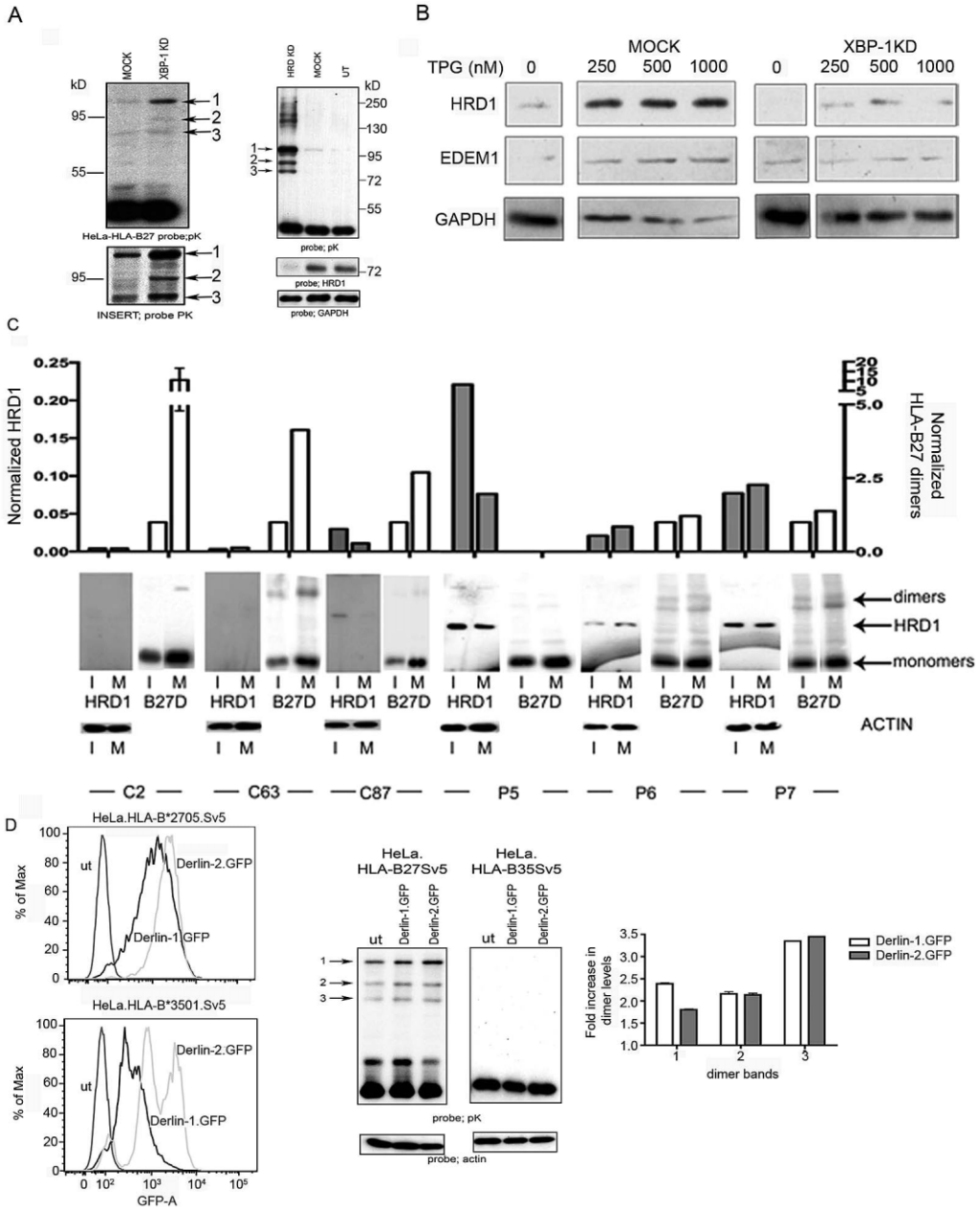

Figure 4. X-box binding protein 1 (XBP-1), hydroxymethylglutaryl-coenzyme A reductase degradation 1 (HRD1), and derlins 1 and 2 participate in HLA–B27 dimer degradation. **A,** Degradation of HLA–B27 is dependent on the XBP-1 pathway. Left, Inhibition of XBP-1 in HeLa–B27 cells via shRNA resulted in enhanced dimerization of HLA–B27. Insert shows the dimers after longer exposure. Right, HRD1 inhibition in HeLa–B27 cells via shRNA prevented HLA–B27 dimer ER stress–induced degradation (ERAD) when compared to mock transduction with a control shRNA (shLuc). Immunoblotting of lysates demonstrated down-regulation of HRD1. **B,** HRD1 and EDEM1 depend on XBP-1 for ER stress induction. Inhibition of XBP-1 did not lead to induction of HRD1 and EDEM1 following ER stress induction with TPG compared to shLuc mock control cells. **C,** Levels of HRD1- and HC10-reactive HLA–B27 dimer were quantified in both immature (I) and mature (M) dendritic cells generated from HLA–B27–positive controls (C) and ankylosing spondylitis (AS) patients (P). HRD1 levels were elevated in dendritic cells from the AS patients. Shaded bars represent normalized HRD1 levels; open bars represent normalized B27 dimer (D) levels. **D,** Derlins 1 and 2 can participate in HLA–B27 dimer ERAD. Left, Expression of derlin 1 and derlin 2 green fluorescent protein (GFP) fusion proteins. Middle, HeLa–B27 cells were transduced with derlin 1 and derlin 2 GFP–tagged proteins, which act as dominant-negative inhibitors of the respective derlin activities. Immunoblotting revealed that both derlin 1 and derlin 2 could modestly enhance HLA–B27 dimer formation, leading to the enhanced detection of dimers as highlighted by **arrows 1, 2,** and **3**. Right, Quantitation of dimer bands 1, 2, and 3 reveals a 2–3-fold increase in their detection when derlin 1 and 2 activities are inhibited. See Figure 2 for other definitions.

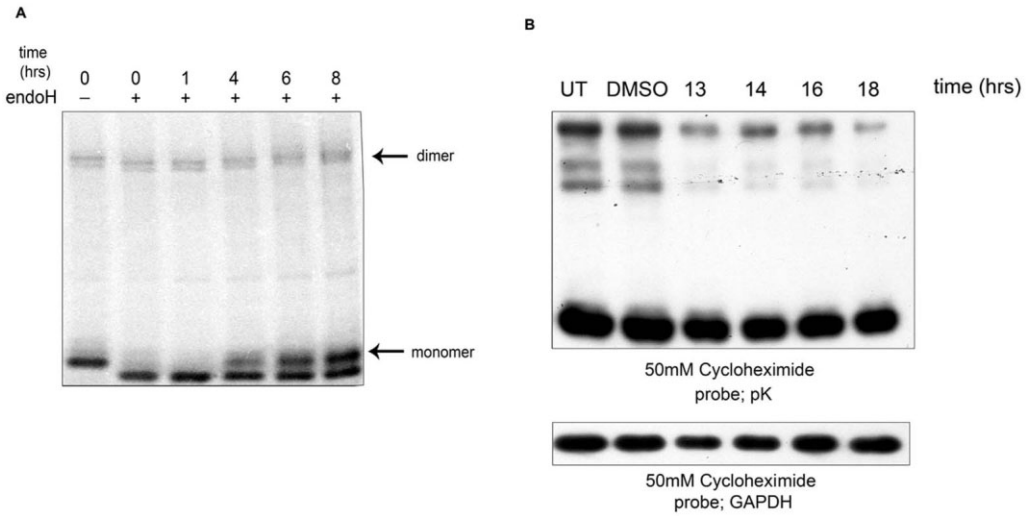

Figure 5. Half-life of HLA–B27 heavy chain dimers. **A,** HLA–B27 dimers have a prolonged half-life. HeLa–B27Sv5 cells were metabolically labeled, chased, and immunopecipitated with pK antibody. HLA–B27 dimers were apparent at 8 hours of chase. **B,** HLA–B27 dimers have a half-life in excess of 16 hours. HeLa–B27Sv5 cells were treated with 50 μM cycloheximide, and dimer levels were detected by immunoblotting of lysates resolved by nonreducing sodium dodecyl sulfate–polyacrylamide gel electrophoresis. Endo H = endoglycosidase H; UT = untreated.

well studied, although HC10-reactive HLA–B27 dimers have been reported to have a half-life of ~2 hours (31). Using our controlled expression system of HLA–B27 we were able to determine the duration of all populations of dimers.

We metabolically labeled HeLa–B27 cells for 15 minutes with ^{35}S-Cys/Met before chasing for 0, 2, 4, 6, and 8 hours and immunoprecipitating with the anti-Sv5 pK antibody. Pulse chase analysis revealed that dimers were long-lived and evident up to 8 hours (Figure 5A). To further assess the half-life of HLA–B27 dimers, we treated cells with the protein synthesis inhibitor cycloheximide (50 μM) and determined dimer levels by immunoblotting. Again this analysis revealed that HLA–B27 dimers were extremely long-lived, with detectable levels remaining 18 hours after cycloheximide treatment (Figure 5B). Therefore, at steady-state levels, HLA–B27 dimers exhibit a prolonged lifetime and appear to be resistant to steady-state degradation pathways.

Enhancement of ERAD of HLA–B27 dimers by pharmacologic induction of the UPR. Our data indicated that induction of ER stress could aid in dimer removal and could potentially be used as a therapeutic intervention strategy. If EDEM1 and/or other proteins that are up-regulated during ER stress are involved in ERAD of HLA–B27 dimers, we hypothesized that induction of the UPR should enhance the removal of HLA–B27 dimers. To test this, HeLa–B27.Sv5 cells were incubated with pharmacologic agents known to induce the UPR, such as TUN, TPG, and MG132 (32). Immunoblotting revealed significantly fewer HLA–B27 dimers (Figure 6A), suggesting that ER stress–induced ERAD was regulating dimer levels.

We then determined whether ER stress reduced the half-life of dimers by performing kinetic and pulse chase analyses. A kinetic study of the effects of these drugs revealed initial enhanced dimerization, as might be expected from their ability to inhibit normal folding processes, but this was followed by dimer disappearance (Figures 6B and C and Guiliano DB, et al: unpublished observations). For pulse chase analysis, cells were metabolically labeled and at the point of chase, were incubated with TUN. Following such treatment, dimers were indeed degraded far more rapidly, disappearing within 8–12 hours posttreatment (Figure 6C). Previously, we demonstrated that changes within the 1–2 hours of maturation can affect the ability of MHC class I molecules to dimerize (23). It was possible that dimer levels could be modulated by the effects of these drugs on the maturation rates of the HLA–B27 monomer, but pulse chase analysis in the presence of TPG and TUN did not reveal any alterations to the maturation phenotype following ER stress induction during the first 4 hours. However, TUN appeared to enhance the maturation rate markedly, while TPG had little if any effect (Figure 6D). Therefore, induction of ER stress using a pharmacologic approach can modulate levels of aberrant misfolded MHC class I molecules.

DISCUSSION

In the present study we have defined a role of EDEM1 in the degradation pathway of HLA–B27 di-

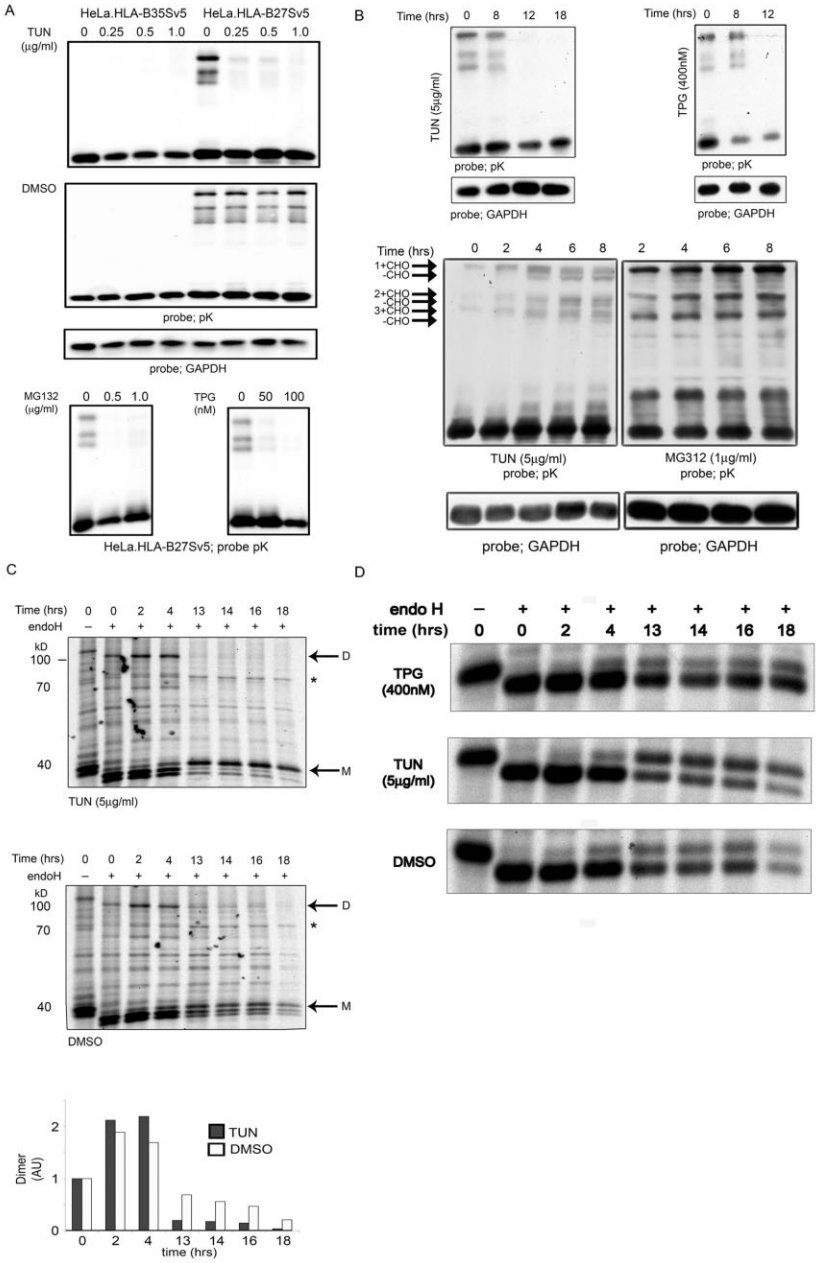

Figure 6. Incubation with unfolded protein response–inducing drugs leads to loss of HLA–B27 dimers. **A,** Treatment with tunicamycin (TUN), TPG, and MG132 led to loss of HLA–B27 dimers. **B,** Top, Treatment with TUN and TPG resulted in disappearance of dimers after 8 hours. Bottom, ER stress–inducing drugs exhibited a biphasic effect, with TUN and MG132 treatment leading to the accumulation of dimers up to 8 hours and TUN treatment resulting in the appearance of glycan-free (−CHO) forms of dimers. **C,** TUN enhances the rate of dimer degradation. Top and middle, HLA–B27 cells were labeled with ^{35}S-Cys/Met and then chased in the presence of 5 μg/ml TUN (top) or in the absence of TUN (middle). Cells were chased for 0, 2, 4, 13, 14, 16, and 18 hours and immunoprecipitated for MHC class I heavy chain with pK antibody. Dimers (D) and monomers (M) are highlighted. **Asterisk** denotes BiP. Note that dimers were not apparent after 4 hours of chase (top). Bottom, The presence of dimers at each time point was assessed quantitatively. **D,** The maturation rate of HLA–B27 as determined by pulse chase analysis was not substantially affected by ER stress–inducing drugs (TPG and TUN). See Figure 2 for other definitions.

meric molecules. The XBP-1–induced ERAD of HLA–B27 dimers involves EDEM1, the E3 ubiquitin ligase HRD1, and the adaptor proteins derlins 1 and 2 (Figure 4). EDEM1 shows specific affinity for HLA–B27 dimers as well as binding to misfolded monomers (Figures 2 and 3).

The induction of ERAD via the UPR has been demonstrated to lead to the degradation of misfolded

proteins (33). UPR-induced ERAD appears to target misfolded polypeptides in preference to folded monomers, and this could be explained in part by the activity of EDEM1. How EDEM1 distinguishes such structures remains unresolved, but could involve interactions with calnexin and/or BiP. EDEM1 was originally proposed to act on misfolding substrates through its proposed mannosidase activity (15–17). However, our findings demonstrate that the mannosidase-active site of EDEM1 is not necessary for substrate interactions (Figure 3C) and suggest that the glycosylation status of this substrate does not influence its interaction with EDEM1. These results are consistent with previously reported observations on EDEM1 interactions in a study using the misfolding α_1-antitrypsin–null Hong Kong protein model (18).

Our results strongly suggest that HLA–B27 dimers are long-lived. Relatively little is known regarding the half-life and duration of such aberrant conformers. It has been proposed that HC10-reactive dimers have a half-life of ~2 hours (31). However, in our system HLA–B27 expression was controlled and used a C-terminally tagged epitope, which enabled us to perform an unbiased analysis of dimeric populations. It is possible that dimer duration and expression could be affected by additional factors. Recently, ER aminopeptidase 1 (ERAP-1), which trims MHC class I–associated peptides (34), has also been found to be associated with AS (3). The peptide trimming activity could be altered by ERAP-1 polymorphisms associated with AS or by increased expression levels (35), which could generate unstable peptides similar to those observed in ERAP-1–knockout cells (36). An altered peptide subset could lead to MHC class I misfolding, increasing the propensity for HLA–B27 to dimerize and potentially overload the ERAD cell machinery. Recently, a poor supply of peptides was postulated to participate in the expression of cell surface HLA–B27 dimeric conformers (37). Thus, it is entirely possible that the peptide repertoire could participate in the expression of aberrant ER-resident or plasma membrane–associated HLA–B27 conformers.

The present findings have 3 potentially important implications. First, if misfolding and aggregation of HLA–B27 cause the associated inflammatory diseases, then they could be targeted for therapeutic intervention, as proposed for other conformational diseases, such as α_1-antitrypsin deficiency (38). HRD1 activity has been implicated in such disorders (39), and our demonstration that HRD1 expression, and possibly activity, correlates with disease suggests that this pathway may have an important role in how these conformers are handled in AS. Although we demonstrated that HRD1 and EDEM1 participate in the degradation of HLA–B27 dimers and that this pathway may be activated in AS, it is possible that there are differences in these pathways when comparing ex vivo DC–expressing physiologic levels of MHC class I molecules versus transfected cell lines, and this will require further investigation.

Second, EDEM1 and engagement of the HRD1–SEL1 complex appear to be the rate-limiting steps in the degradation of pathogenic disulfide-bonded dimers of HLA–B27. It has previously been postulated that the resolution of disulfide bonds of HLA–B27 homodimers determined the rate of their degradation (31); however, at steady state these molecules are far more long-lived and stable than originally proposed.

Third, the degradation of HLA–B27 dimers offers the potential for therapeutic targeting by manipulating the ER stress response and induction of the ERAD pathway. Our study demonstrates that the ER stress pathway can be manipulated to modulate dimer expression. The use of ER stress–inducing drugs highlights this proof-of-principle application, with dimers becoming less apparent following the use of such ER stress–inducing drugs (Figure 6). Pulse chase analysis with the drugs administererd at the point of chase demonstrated that the heavy chain can still mature slowly and that maturation is not altered significantly to account for the reduced detection of dimeric HLA–B27 populations (Figure 6D). Thus, the observed effects of these drugs on dimer levels are not due to their effects on folding. These agents should, in theory, perturb folding and as such, cause an accumulation of dimers. However, kinetic studies demonstrated a biphasic action of the drugs, with a brief accumulation of dimers in the early stages (0–8 hours) (Figure 6B), which then decline at later time points, correlating with the induction of HRD1 (Guiliano DB, et al: unpublished observations). Therefore, the initial effect of ER stress–inducing drugs is to interfere with protein folding, with the accumulation of misfolding protein triggering ER stress pathways.

The spondyloarthritides have been hypothesized to be disorders resulting from HLA–B27 misfolding, with dimerization contributing to the disease process (4,40). Understanding the factors that contribute to the misfolding of HLA–B27 could have an impact on future treatment approaches. The present findings suggest that modulation of ER stress could offer a novel therapeutic intervention point. Drugs modulating ER stress responses are already under clinical development and testing for the treatment of multiple myelomas (41,42). These could also be tested and, if effective, repurposed, for the treatment of HLA–B27–associated diseases as well as other disorders associated with protein misfolding.

ACKNOWLEDGMENTS

We thank Drs. H. Ploegh, J. Neefjes, and P. Lehner for supplying reagents.

AUTHOR CONTRIBUTIONS

All authors were involved in drafting the article or revising it critically for important intellectual content, and all authors approved the final version to be published. Dr. Antoniou had full access to all of the data in the study and takes responsibility for the integrity of the data and the accuracy of the data analysis.

Study conception and design. Guiliano, Lenart, Hebert, Powis, Antoniou.

Acquisition of data. Guiliano, Fussell, Lenart, Tsao, Nesbeth, Fletcher, Campbell, Yousaf, Williams, Santos, Cameron, Towers, Kellam, Powis, Antoniou.

Analysis and interpretation of data. Guiliano, Fussell, Lenart, Yousaf, Gould, Powis, Antoniou.

REFERENCES

1. Schlosstein L, Terasaki PI, Bluestone R, Pearson CM. High association of an HL-A antigen, W27, with ankylosing spondylitis. N Engl J Med 1973;288:704–6.
2. Brewerton DA, Hart FD, Nicholls A, Caffrey M, James DC, Sturrock RD. Ankylosing spondylitis and HL-A 27. Lancet 1973; 1:904–7.
3. Burton PR, Clayton DG, Cardon LR, Craddock N, Deloukas P, Duncanson A, et al. Association scan of 14,500 nonsynonymous SNPs in four diseases identifies autoimmunity variants. Nat Genet 2007;39:1329–37.
4. Antoniou AN, Lenart I, Guiliano DB. Pathogenicity of misfolded and dimeric HLA-B27 molecules. Int J Rheumatol 2011;2011: 486856.
5. Tran TM, Satumtira N, Dorris ML, May E, Wang A, Furuta E, et al. HLA-B27 in transgenic rats forms disulfide-linked heavy chain oligomers and multimers that bind to the chaperone BiP. J Immunol 2004;172:5110–9.
6. Kollnberger S, Bird L, Sun MY, Retiere C, Braud VM, McMichael A, et al. Cell-surface expression and immune receptor recognition of HLA–B27 homodimers. Arthritis Rheum 2002;46:2972–82.
7. Layh-Schmitt G, Colbert RA. The interleukin-23/interleukin-17 axis in spondyloarthritis [review]. Curr Opin Rheumatol 2008;20: 392–7.
8. Mear JP, Schreiber KL, Munz C, Zhu X, Stevanovic S, Rammensee HG, et al. Misfolding of HLA-B27 as a result of its B pocket suggests a novel mechanism for its role in susceptibility to spondyloarthropathies. J Immunol 1999;163:6665–70.
9. Kozutsumi Y, Segal M, Normington K, Gething MJ, Sambrook J. The presence of malfolded proteins in the endoplasmic reticulum signals the induction of glucose-regulated proteins. Nature 1988; 332:462–4.
10. Welihinda AA, Tirasophon W, Kaufman RJ. The cellular response to protein misfolding in the endoplasmic reticulum. Gene Expr 1999;7:293–300.
11. Zhang K, Kaufman RJ. The unfolded protein response: a stress signaling pathway critical for health and disease. Neurology 2006;66 Suppl 1:S102–9.
12. Foti DM, Welihinda A, Kaufman RJ, Lee AS. Conservation and divergence of the yeast and mammalian unfolded protein response: activation of specific mammalian endoplasmic reticulum stress element of the grp78/BiP promoter by yeast Hac1. J Biol Chem 1999;274:30402–9.
13. Yoshida H, Matsui T, Yamamoto A, Okada T, Mori K. XBP1 mRNA is induced by ATF6 and spliced by IRE1 in response to ER stress to produce a highly active transcription factor. Cell 2001; 107:881–91.
14. Lee AH, Iwakoshi NN, Glimcher LH. XBP-1 regulates a subset of endoplasmic reticulum resident chaperone genes in the unfolded protein response. Mol Cell Biol 2003;23:7448–59.
15. Hosokawa N, Wada I, Hasegawa K, Yorihuzi T, Tremblay LO, Herscovics A, et al. A novel ER α-mannosidase-like protein accelerates ER-associated degradation. EMBO Rep 2001;2: 415–22.
16. Molinari M, Calanca V, Galli C, Lucca P, Paganetti P. Role of EDEM in the release of misfolded glycoproteins from the calnexin cycle. Science 2003;299:1397–400.
17. Oda Y, Hosokawa N, Wada I, Nagata K. EDEM as an acceptor of terminally misfolded glycoproteins released from calnexin. Science 2003;299:1394–7.
18. Cormier JH, Tamura T, Sunryd JC, Hebert DN. EDEM1 recognition and delivery of misfolded proteins to the SEL1L-containing ERAD complex. Mol Cell 2009;34:627–33.
19. Burr ML, Cano F, Svobodova S, Boyle LH, Boname JM, Lehner PJ. HRD1 and UBE2J1 target misfolded MHC class I heavy chains for endoplasmic reticulum-associated degradation. Proc Natl Acad Sci U S A 2011;108:2034–9.
20. Burr ML, van den Boomen DJ, Bye H, Antrobus R, Wiertz EJ, Lehner PJ. MHC class I molecules are preferentially ubiquitinated on endoplasmic reticulum luminal residues during HRD1 ubiquitin E3 ligase-mediated dislocation. Proc Natl Acad Sci U S A 2013;110:14290–5.
21. Wilson SJ, Tsao EH, Webb BL, Ye H, Dalton-Griffin L, Tsantoulas C, et al. X box binding protein XBP-1s transactivates the Kaposi's sarcoma-associated herpesvirus (KSHV) ORF50 promoter, linking plasma cell differentiation to KSHV reactivation from latency. J Virol 2007;81:13578–86.
22. Groisman B, Shenkman M, Ron E, Lederkremer GZ. Mannose trimming is required for delivery of a glycoprotein from EDEM1 to XTP3-B and to late endoplasmic reticulum-associated degradation steps. J Biol Chem 2011;286:1292–300.
23. Antoniou AN, Ford S, Taurog JD, Butcher GW, Powis SJ. Formation of HLA-B27 homodimers and their relationship to assembly kinetics. J Biol Chem 2004;279:8895–902.
24. Lenart I, Guiliano DB, Burn G, Campbell EC, Morley KD, Fussell H, et al. The MHC class I heavy chain structurally conserved cysteines 101 and 164 participate in HLA-B27 dimer formation. Antioxid Redox Signal 2011;16:33–43.
25. Molinari M, Galli C, Piccaluga V, Pieren M, Paganetti P. Sequential assistance of molecular chaperones and transient formation of covalent complexes during protein degradation from the ER. J Cell Biol 2002;158:247–57.
26. Saeed M, Suzuki R, Watanabe N, Masaki T, Tomonaga M, Muhammad A, et al. Role of the endoplasmic reticulum-associated degradation (ERAD) pathway in degradation of hepatitis C virus envelope proteins and production of virus particles. J Biol Chem 2011;286:37264–73.
27. Yamamoto K, Suzuki N, Wada T, Okada T, Yoshida H, Kaufman RJ, et al. Human HRD1 promoter carries a functional unfolded protein response element to which XBP1 but not ATF6 directly binds. J Biochem 2008;144:477–86.
28. Smith MH, Ploegh HL, Weissman JS. Road to ruin: targeting proteins for degradation in the endoplasmic reticulum. Science 2011;334:1086–90.
29. Lilley BN, Ploegh HL. A membrane protein required for dislocation of misfolded proteins from the ER. Nature 2004;429:834–40.
30. Oda Y, Okada T, Yoshida H, Kaufman RJ, Nagata K, Mori K. Derlin-2 and Derlin-3 are regulated by the mammalian unfolded protein response and are required for ER-associated degradation. J Cell Biol 2006;172:383–93.
31. Dangoria NS, DeLay ML, Kingsbury DJ, Mear JP, Uchanska-Ziegler B, Ziegler A, et al. HLA-B27 misfolding is associated with aberrant intermolecular disulfide bond formation (dimerization) in the endoplasmic reticulum. J Biol Chem 2002;277:23459–68.

32. Mu TW, Ong DS, Wang YJ, Balch WE, Yates JR 3rd, Segatori L, et al. Chemical and biological approaches synergize to ameliorate protein-folding diseases. Cell 2008;134:769–81.
33. Friedlander R, Jarosch E, Urban J, Volkwein C, Sommer T. A regulatory link between ER-associated protein degradation and the unfolded-protein response. Nat Cell Biol 2000;2:379–84.
34. Saric T, Chang SC, Hattori A, York IA, Markant S, Rock KL, et al. An IFN-γ-induced aminopeptidase in the ER, ERAP1, trims precursors to MHC class I-presented peptides. Nat Immunol 2002;3:1169–76.
35. Campbell EC, Fettke F, Bhat S, Morley KD, Powis SJ. Expression of MHC class I dimers and ERAP1 in an ankylosing spondylitis patient cohort. Immunology 2011;133:379–85.
36. Hammer GE, Gonzalez F, James E, Nolla H, Shastri N. In the absence of aminopeptidase ERAAP, MHC class I molecules present many unstable and highly immunogenic peptides. Nat Immunol 2007;8:101–8.
37. McHugh K, Rysnik O, Kollnberger S, Shaw J, Utriainen L, Al-Mossawi MH, et al. Expression of aberrant HLA-B27 molecules is dependent on B27 dosage and peptide supply. Ann Rheum Dis 2014;73:763–70.
38. Hidvegi T, Ewing M, Hale P, Dippold C, Beckett C, Kemp C, et al. An autophagy-enhancing drug promotes degradation of mutant α1-antitrypsin Z and reduces hepatic fibrosis. Science 2010;329:229–32.
39. Kaneko M, Koike H, Saito R, Kitamura Y, Okuma Y, Nomura Y. Loss of HRD1-mediated protein degradation causes amyloid precursor protein accumulation and amyloid-β generation. J Neurosci 2011;30:3924–32.
40. Colbert RA. HLA-B27 misfolding: a solution to the spondyloarthropathy conundrum? Mol Med Today 2000;6:224–30.
41. Lee AH, Iwakoshi NN, Anderson KC, Glimcher LH. Proteasome inhibitors disrupt the unfolded protein response in myeloma cells. Proc Natl Acad Sci U S A 2003;100:9946–51.
42. Obeng EA, Carlson LM, Gutman DM, Harrington WJ Jr, Lee KP, Boise LH. Proteasome inhibitors induce a terminal unfolded protein response in multiple myeloma cells. Blood 2006;107:4907–16.